論文 / 著書情報
Article / Book Information

Title	Determination of carrier mobility of semiconductor layer in organic metal-insulator-semiconductor diodes by displacement current and electric-field-induced optical second-harmonic generation measurements
Authors	Taishi Noma, Dai Taguchi, Takaaki Manaka, Hong Lin, MITSUMASA IWAMOTO
Citation	Organic Electronics, 43, 70-76
Pub. date	2017, 1
DOI	http://dx.doi.org/10.1016/j.orgel.2017.01.004
Creative Commons	See next page.
Note	This file is author (final) version.

License

Determination of carrier mobility of semiconductor layer in organic metal-insulator-semiconductor diodes by displacement current and electric-field-induced optical second-harmonic generation measurements

Taishi Noma [a,b], Dai Taguchi [a], Takaaki Manaka [a], Hong Lin [b], Mitsumasa Iwamoto [a,*]

[a] *Department of Electrical and Electronic Engineering, Tokyo Institute of Technology, 2-12-1 O-okayama, Meguro-ku, Tokyo 152-8552, Japan*

[b] *State Key Laboratory of New Ceramics and Fine Processing, School of Materials Science and Engineering, Tsinghua University, Beijing 100084, P. R. China*

E-mail address: iwamoto@pe.titech.ac.jp

ABSTRACT

A novel method for determining carrier mobility of semiconductor layer in thin-film organic metal-insulator-semiconductor (MIS) diodes is proposed, where displacement current measurement (DCM) is used in combination with electric-field-induced optical second-harmonic generation (EFISHG) measurement. EFISHG signals generated from the semiconductor layer probe the electric field caused by carriers moving in the semiconductor layer of MIS diodes. On the other hand, DCM signals generated in accordance with the time derivative of induced charge on metal electrode well identify the transit time of carriers across the semiconductor layer. By using Au/pentacene/polyimide (PI)/ indium-tin-oxide (ITO) diodes, we experimentally determined the carrier mobility of the pentacene layer. Results and analysis showed that step-voltage application to MIS diodes is suitable for the use of this proposed method.

1. Introduction

Recently, the carrier mobility of organic semiconductor layer in organic devices has attracted much attention in electronics, because the performance of organic devices such as transistors, diodes, electroluminescence devices and others depends on the carrier mobility. Till now, carrier extraction by linearly increasing voltage (CELIV) [1–6] method and charge-retraction time-of-flight (TOF) measurement [7] have been utilized for determining carrier mobility in semiconductor layer of metal-insulator-semiconductor (MIS) diodes. These measurements are basically displacement current measurements (DCM) [8], and transfer of carriers in semiconductor layer is recorded as Maxwell's transient currents by applying ramp voltages. Carrier transit time t_r is determined from the trace of transient current, and the carrier mobility μ is evaluated using the relationship of

$$\int_0^{t_r} \mu E_1 \, dt = d_1, \tag{1}$$

assuming that carriers are conveyed by electric field E_1 in the semiconductor layer. Here, d_1 is the thickness of the semiconductor layer, and E_1 is the sum of external field E_{1lap} and space charge field E_{1s}, $E_1 = E_{1lap} + E_{1s}$. Conventionally, the electric field E_1 is assumed constant during the measurement, and the carrier mobility is determined as $\mu = \frac{{d_1}^2}{V_1 t_r}$, under the assumption that space charge field E_{1s} formed by the interface charge Q_s can be neglected. That is, the applied voltage across the semiconductor layer is assumed $V_1 = E_1 d_1 = E_{1lap} d_1$. Also it is assumed that upon application of external field E_1 (>0) at $t = 0$, carriers immediately start to move in the semiconductor layer by the force of external electric field. However, this is not the case when we talk about carrier mobility in thin film MIS diodes. The carriers are injected from an electrode, and they are accumulated as excessive charges at the semiconductor/insulator interface, to form space charge field. Therefore, we need to use a method that can directly measure the local electric field in the semiconductor layer and can also determine the actual carrier transit time. Recently, electric-field-induced optical second-harmonic generation (EFISHG) measurement has been developed to directly observe electric field in organic devices [9–13]. By using this EFISHG method, we can directly measure the evolution of electric field E_1 being formed in the organic layer with time, by probing SH light generated from the organic layer. We therefore anticipate that the carrier mobility μ can be determined using the relationship of

Eq. (1) with taking into account the contribution of space charge field E_s, if we can determine carrier transit time t_r accurately.

In this study, we propose a method for the determination of carrier mobility in the semiconductor layer in organic metal-insulator-semiconductor (MIS) diodes by using DCM and EFISHG measurements, with taking into account the time evolution of electric field in the semiconductor layer. Here, we use Au/pentacene/polyimide (PI)/indium-tin-oxide (ITO) diodes, where pentacene and polyimide are serving as semiconductor layer and electrical insulating layer, respectively. We then discuss the determination of carrier mobility μ, using the DCM and EFISHG method, in terms of the waveform of applied voltages.

2. Experimental methods

Fig. 1 (a) shows the sample structure used here. Firstly, we spin-coated polyimide precursor film of cyclobutanedianhydride-2,2-bis(4-amino-phenoxyphenyl)propane (CBDA-BAPP) with a thickness of 100 nm (= d_2) onto an ITO substrate. After that, the deposited polyimide precursor film was thermally imidized in an oven at 260 °C for two hours to produce a polyimide (PI) film. Subsequently, 100 nm (= d_1) thickness pentacene was thermally deposited on the substrate coated with the PI film. Finally, Au electrode was evaporated in a vacuum. The working electrode area was 3.1 mm^2. Relative dielectric constants of pentacene and polyimide are $\varepsilon_1 = 4.2$ [13] and $\varepsilon_2 = 3.3$ [14], respectively. Thus capacitances are $C_1 = 1.15$ nF and $C_2 = 0.91$ nF, respectively.

In the DCM, an external voltage displayed in Fig. 1 (c) and (d) was applied to the Au electrode with reference to the ITO electrode grounded, as illustrated in Fig. 1 (a). On the other hand, in the EFISHG measurement we applied a laser pulse with a wavelength of 860 nm to the pentacene layer through the transparent ITO electrode, and probed the SH light generated at a wavelength of 430 nm. Here, we used Nd:YAG laser (repetition rate 10 Hz, average power 1 mW/cm^2, duration 4 ns), and the timing of laser pulse was chosen in a manner as displayed in Fig. 1 (c) and (d). Pentacene is molecularly symmetric, and no ordinary SH generation due to second order nonlinear polarization is anticipated under dipolar approximation [15]. However, SH is activated in the presence of electrostatic field, due to the enhancement of the third order nonlinear polarization. This SHG is so-called the

electric-field-induced optical second-harmonic generation (EFISHG). Noteworthy that this SH enhancement is material dependent and is strongly dependent on the electro-magnetic wavelength, and we set the laser wavelength at 860 nm (SH wavelength 430 nm) to directly probe electric field in pentacene [12].

In a case that the density of carriers in bulk semiconductor layer is very low and it can be neglected compared to the density of carriers accumulated at the insulator/semiconductor interface, the electric field in pentacene layer E_1 is calculated as

$$E_1 = E_{1lap} + E_{1s} = \frac{1}{d_1}\frac{C_2}{C_1+C_2}V_{ex} - \frac{1}{d_1}\frac{Q_s}{C_1+C_2}, \quad (2)$$

by modeling our MIS diode as a double layer dielectric system [12]. Here, Q_s represents the interface charge at the pentacene/PI interface. Therefore, when we apply a bias voltage to the Au electrode, the electric field formed in the pentacene layer is given as the sum of the Laplace field E_{1lap} that appears in the absence of interface charge Q_s (=0), i.e., the first term of Eq. (2), and the space charge field E_{1s} generated due to the presence of interfacial charge Q_s (≠0), i.e., the second term of Eq. (2). Fig. 1 (b) shows the SH intensity-voltage characteristics obtained under the Laplace-field condition, experimentally by choosing t_d = 90 ns under step-voltage application (see Fig. 1 (c)). The square root of the enhanced SH intensity is linearly proportional to the electric field E_1 in the pentacene layer according to Eq. (3), and we can convert the experimental SH intensity to the electric field E_1 using Fig. 1 (b).

$$I_{SHG} \propto \left|\varepsilon_0\chi^{(3)} : E_1(0)E_1(\omega)E_1(\omega)\right|^2 \propto |E_1(0)|^2. \quad (3)$$

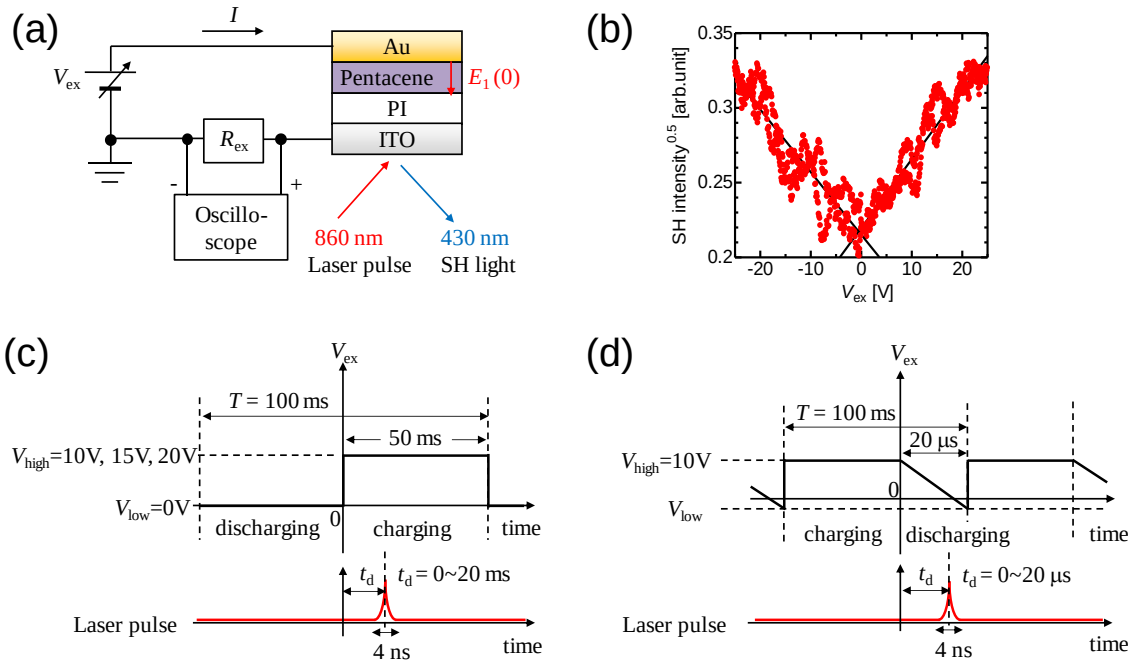

Fig. 1. (a) Sample structure. (b) SH-V characteristics. (c) Waveform of applied external voltage V_{ex} under step-voltage application and (d) under ramp-voltage application.

3. Results

3.1. Determination of carrier mobility by step-voltage application

We applied step voltages with V_{high} = 10 V, 15 V, and 20 V, in a manner as illustrated in Fig. 1 (c) and Fig. 2 (a), and measured the transient current I flowing through the external circuit by the DCM and the electric field E_1 in pentacene layer by the EFISHG. Fig. 2 (a) shows the observed current I and the electric field E_1. As we can see in the figure, the current I gradually increases and saturates. After that it gradually decays. We divided the experimental result into 4 regions as shown in Fig. 2 (a). In region (i), a very sharp current with exponential decay should be observed due to the electrode charging by the application of step voltage, if the pentacene and PI layers serve as dielectric material. This current is given by using an exponential decaying function;

$$I_0 = \frac{V_{ex}}{R_{ex}} \exp\left(-\frac{t}{\tau_1}\right), \tag{4}$$

where R_{ex} is the external resistance of the circuit (R_{ex} = 100 Ω). However, the observed transient current I in region (i) was different from the current I_0, given by Eq. (4), and the recorded electric field E_1 was low and nearly constant, possibly owing to the lead

resistance of the external circuit, the response time of our ammeter, and so forth. In region (ii), the current I decays but the recorded electric field E_1 increases, suggesting that charges are accumulated on the Au and ITO electrodes. It is instructive to note that the electric field E_1 measured by the EFISHG in region (i) and (ii) is the Laplace field E_{1lap} formed in the pentacene layer due to the charges accumulated on the electrodes (see the first term of Eq. (2)), without accompanying carrier injection from Au and ITO electrodes. To confirm this situation, we calculated the electric field E_{1lap} across the pentacene layer generated due to accumulated charges on electrodes by using the following relation:

$$\int_0^t I\,dt = C_1 E_{1lap} d_1, \tag{5}$$

assuming that PI layer is working as an ideal insulator. Results are plotted in Fig. 2 (b) by a dotted line. As we can see in the figure, in region (i) and (ii), the calculated electric field E_{1lap} increases in the way similar to the trace of the electric field E_1 measured by the EFISHG, whereas in region (iii), the calculated E_{1lap} deviates from the E_1 with time. This result indicates that accumulated charges on the Au electrodes enter into the pentacene layer, to accumulate at the pentacene/PI interface (see the second term of Eq. (2)). Furthermore, as shown in Fig. 2 (c), the experimental transient current I was greater than the current I_0' only in region (iii). Here the I_0' was calculated using the relation Eq. (4) with a fitting parameter $\tau_1 = R_{ex}C_1C_2/(C_1+C_2)$ = 42 ns, with taking into account the delay of the response of 30 ns. This result indicates that pentacene is serving as an insulator and only electrode charging happens in region (i), (ii) and (iv). At the end of region (iii), the injected charge reaches the pentacene/PI interface and the carrier motion is stopped. Therefore, in region (iv), only electrode charging current flows in the same way as region (ii). We therefore argue that carriers transit in region (iii) with a transit time t_r of t_{34} - t_{23}, and the hole mobility was calculated using the relationship between mobility μ and electric field E_1 given by (the detailed calculation is shown in Appendix)

$$\mu = \frac{d_1}{\int_{t_{23}}^{t_{34}} E_1(t)dt}. \tag{6}$$

Here, $t = t_{23}$ is the time corresponding to the beginning of region (iii) and $t = t_{34}$ is the time corresponding to the end of region (iii). The hole mobilities of pentacene obtained at various voltages V_{high} were approximately 3.0×10^{-4} cm^2/Vs, as plotted in Fig. 3.

As mentioned above, we can determine the carrier mobility μ with taking into account

the space charge field E_s and the carrier transit time t_r, by using the results of EFISHG and DCM measurements.

Noteworthy, a charge sheet transportation across the pentacene layer is a possible model to account for the carrier behavior of region (iii), as discussed in the Appendix. According to this model, the observed current I is greater than the current I_0' calculated under Laplace-field conditions, while a charge sheet is transporting across the pentacene layer.

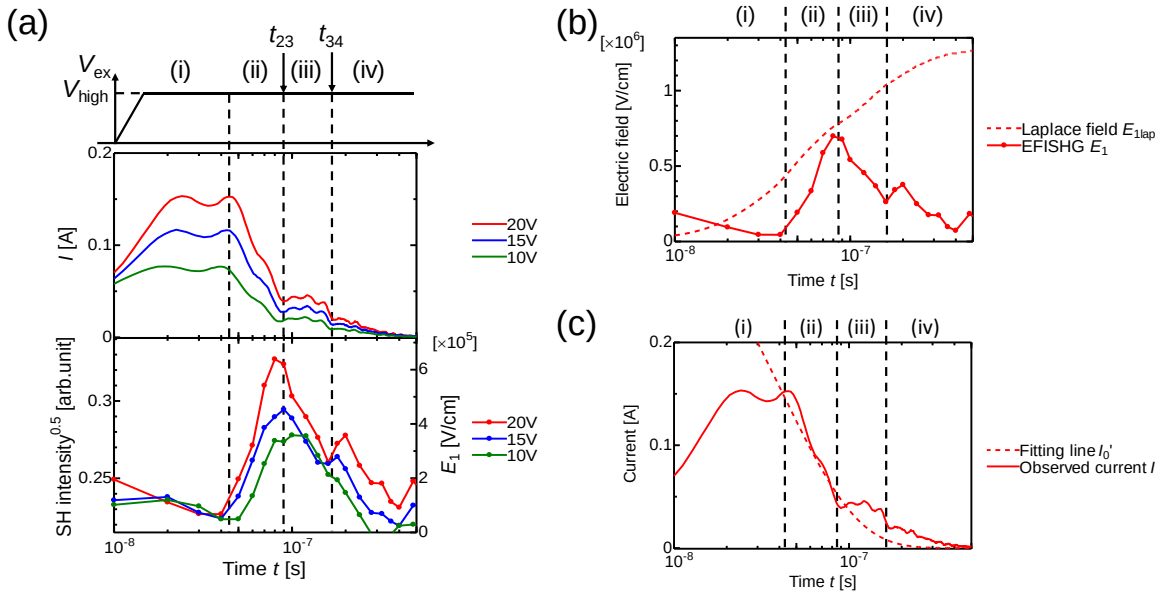

Fig. 2. (a) Transient of the observed current I and square root of SH intensity. (b) Calculated Laplace field E_{1lap} and the electric field E_1 measured by the EFISHG in the pentacene layer (V_{high} = 20 V). (c) Comparison of the charging current I observed by DCM measurement and the theoretical current I_0' calculated under Laplace-field conditions (V_{high} = 20 V).

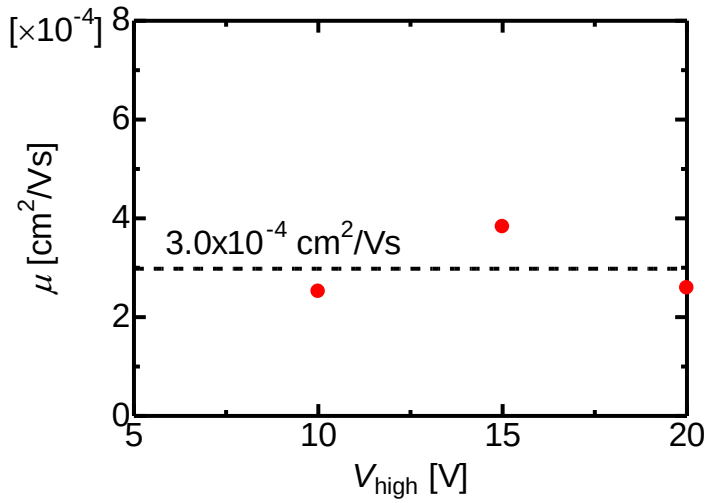

Fig. 3. The hole mobility of pentacene derived from DCM and EFISHG method under a step-voltage application.

3.2. Determination of carrier mobility by ramp-voltage application

We also used the ramp voltage $V_{ex} = V_{high} - At$ ($A > 0$) as shown in Fig. 1 (d) and Fig. 4 (a) for the determination of carrier mobility of the pentacene layer. Here, the sweep rate A was chosen in the region from 2.5×10^5 V/s to 1.5×10^6 V/s. Note that this ramp voltage application was the same as that used in the CELIV method, and our samples were fully charged before the DCM and EFISHG measurement [16]. According to a double-layer dielectric model comprised of a series capacitance of pentacene, C_1 and PI, C_2, discharging current $I(t)$ is given as

$$I(t) = I_0 + \Delta I = \frac{C_1 C_2}{C_1 + C_2}\frac{dV_{ex}}{dt} + \frac{C_2}{C_1 + C_2}\frac{dQ_s}{dt}. \quad (7)$$

The first term I_0 represents the electrode discharging, and the second term ΔI represents the interfacial discharging, where interface charges are allowed to be conveyed only in the direction to the Au electrode owing to the carrier blocking property of PI. Fig. 4 (b) shows the discharging current recorded by the DCM measurement, and we divided the discharging process into 4 regions. In region (i), the discharging current $I(t)$ increased with time, and this current is greater than I_0. This result indicates that the holes that accumulated at the pentacene/PI interface were extracted from this interface and they were then conveyed to the Au electrode. In region (ii), the current $I(t)$ is nearly constant. Interestingly,

this current is given by $I = C_2 \frac{dV_{ex}}{dt}$, as plotted by a dotted line (see Fig. 4 (b)). That is, in this region, pentacene is acting like a conductor. In region (iii), the current $I(t)$ gradually decreased to the I_0. This result indicates that all accumulated carriers were conveyed to the Au electrode by the time corresponding to the end of region (iii). In region (iv), displacement current is nearly constant and it is given by $I = \frac{C_1 C_2}{C_1 + C_2} \frac{dV_{ex}}{dt}$. That is, in this region, both pentacene and PI layers are serving as insulators.

Fig. 4 (c) shows the electric field E_1 in the pentacene layer, which was obtained using the EFISHG measurement. It was found that the electric field E_1 is always negative, indicating that the direction of E_1 is from the pentacene/PI interface to the Au electrode. Solid lines in Fig. 4 (c) indicate the electric fields $E_{1\text{lap}}$, which were plotted using the first term of Eq. (2). Results show that the electric field E_1 gradually approaches the electric field $E_{1\text{lap}}$ with time in region (iii) and (iv), suggesting that the pentacene layer gradually changes into a dielectric layer, in the manner as predicted by the DCM measurement (see Fig. 4 (b)). Similar charge extraction processes can be seen at other sweep rates A.

It is noteworthy that as we measure the discharging process in this measurement, charges accumulated at the interface can leave from the interface in accordance with the ramp voltage in the region $t \geq 0$, which is different from the charging process previously discussed in Section 3.1.

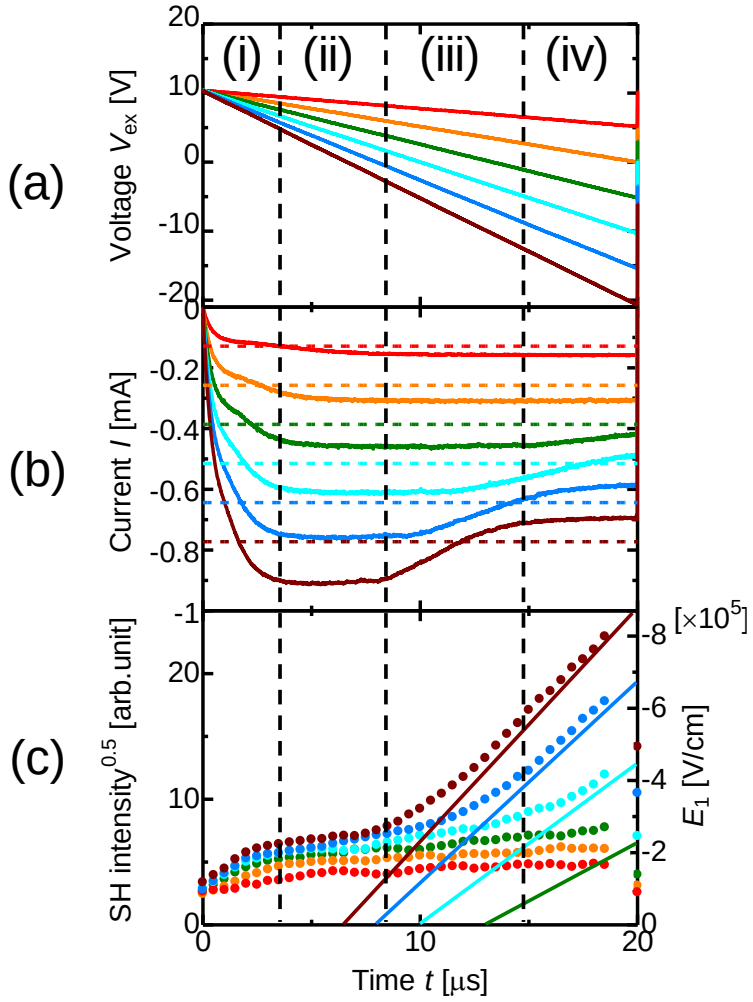

Fig. 4. Transient of (a) external voltage V_{ex}, (b) displacement current (dotted lines represent the calculated displacement current I_0 corresponding to the series capacitance), and (c) electric field E_1 in pentacene layer (solid lines represent Laplace field E_{1lap}). Region (i) to (iv) represent the carrier extraction processes based on the observed transient current when the external voltage V_{ex} was decreased down to -20 V from V_{ex} = 10 V.

In the conventional CELIV method, we assume that E_1 linearly increases with time and it is given by [1]

$$E_1(t) = -\frac{1}{d_1}\frac{C_2}{C_1+C_2}At. \quad (8)$$

Substituting Eq. (8) into Eq. (1), we derive the equation for the determination of carrier mobility

$$\mu = \frac{2{d_1}^2}{A{t_r}^2}\left(1 + \frac{C_1}{C_2}\right) = \frac{2{d_1}^2}{A{t_r}^2}\left(1 + \frac{\varepsilon_1 d_2}{\varepsilon_2 d_1}\right), \quad (9)$$

by integrating the $E_1(t)$ with time in the region $t = 0$ to $t = t_r$ (carrier transit time). Using Eq. (9), we determined the carrier mobility of pentacene as 2.9×10^{-5} cm^2/Vs, by substituting d_1 = 100 nm, d_2 = 100 nm, $\varepsilon_1 = 4.2$, $\varepsilon_2 = 3.3$, $A = 1.5\times10^6$ V/s and $t_r = 4.0$ μs.

Noteworthy that in the conventional CELIV method (called as MIS-CELIV in the MIS-diode configuration), the time t_{max} giving the maximum current peak represents the carrier transit time t_r ($t_{max} = t_r$) in the case of small charge extraction $\Delta I/I_0 < 1$ [1,3,17]. Here ΔI is the deviation of the current peak from the displacement current I_0. In our experiment, $\Delta I/I_0 = 0.22$ when V_{ex} =10 V was decreased down to -20 V (V_{low} = -20 V). Thus we determined that $t_r = t_{max} = 4.0$ μs. The RC response time τ_1 is calculated as $\tau_1 = R_{ex}\frac{C_1C_2}{C_1+C_2} = 0.35\ \mu s$, and this calculated response time is much shorter than the transit time $t_r = 4.0$ μs. That is, we can say that our experimental conditions tentatively meet the requirement of the CELIV method used for the determination of carrier mobility [4]. The carrier mobilities determined at various sweep rates are plotted in Fig. 5. Interestingly, the mobilities are about 10 times smaller than those determined using step-voltage application (see Fig. 3).

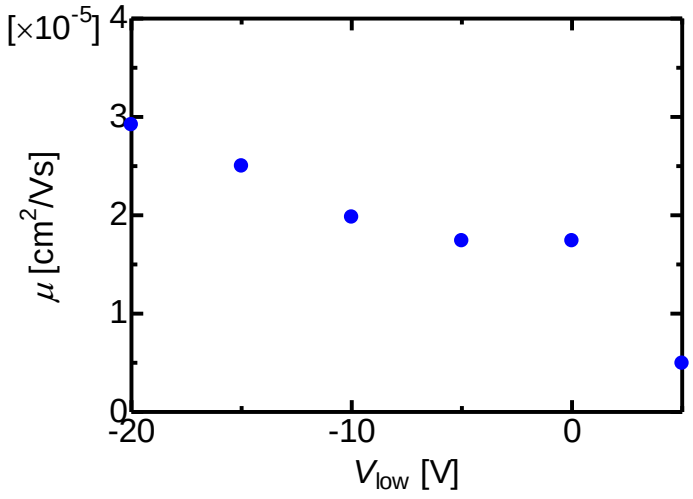

Fig. 5. The hole mobility of pentacene derived from the conventional CELIV method.

4. Discussion

4.1. Determination of transit time t_r using ramp-voltage

We determined the carrier mobility by the CELIV method, as plotted in Fig. 5, but the mobility was much lower than that determined by the DCM method combined with the EFISHG method as plotted in Fig. 3. We studied the details of the reasoning, on focusing the transit time t_r. Fig. 6 (a) shows the applied external voltage V_{ex} and Fig. 6 (b) shows the voltage V_R across the external resistance R_{ex}, given by $R_{ex}I$. Fig. 6 (c) shows the voltage across the pentacene layer V_1, given by E_1d_1. After that, we calculated the ratio of V_1 and V_R as shown in Fig. 6 (d). As plotted in Fig. 6 (d), V_1/V_R is constant over the entire region (i) and (ii), suggesting that pentacene layer serves like a conductor, and Ohmic current flows across the pentacene layer in region (i) and (ii). That is, the carrier transit time across the pentacene layer is very short and the carrier density in the pentacene layer is uniform over the entire region (i) and (ii), and the analysis used in the conventional CELIV method is not available for the determination of carrier mobility in our MIS diodes. In the conventional CELIV method, the transit time is determined from the peak position ($t_r = t_{max}$) of the DCM results, under assumption that $t_r >> \tau_1$, meanwhile the transit time of our MIS diodes is much shorter than circuit RC constant, e.g., τ_1' = 0.71 μs for V_{low} = -20 V. Furthermore, the E_1 (t) in region (i) is given by

$$E_1(t) = \frac{R_1 I}{d_1} = -\frac{R_1 C_2 A}{d_1}\left(1 - \exp\left(-\frac{t}{\tau_1'}\right)\right), \quad (10)$$

where R_1 denotes the resistance of the pentacene layer. The time evolution of E_1 (t) is totally different from Eq. (8). The long response time τ_1' = 0.71 μs suggests that the RC time constant is not given by $\tau_1 = R_{ex}\frac{C_1C_2}{C_1+C_2} = 0.35\ \mu s$. That is, pentacene is not serving as an insulator. On the other hand, in region (iii), the current decreases with a response time of τ_2 = 7.1 μs, but this response time is not corresponding to transit time t_r. Because the electric field E_1 in region (iii) is greater than that in region (i) as shown in Fig. 4 (c), transit time in region (iii) should be shorter than that in region (i). That is, transit time cannot be determined from experimental data in region (iii). Accordingly, the direct observation of E_1 by EFISHG is much helpful for the determination of carrier transit time t_r.

Noteworthy that using a lower sweep rate A will be suitable for the determination of

the transit time t_r, but this is not realistic in actual experiments owing to the decrease of the MDC current that generates in proportion to A (see Eq. (7) and Fig. 4 (b)). Therefore, it is a hard task to determine transit time t_r by using ramp voltage even in a case of DCM method being combined with EFISHG method.

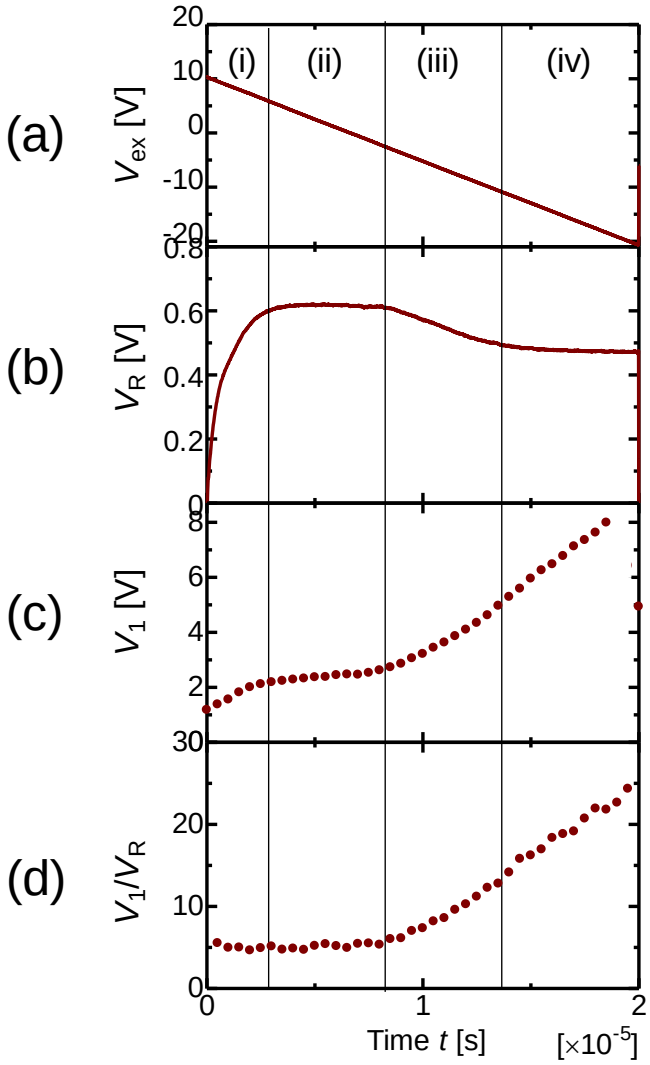

Fig. 6. (a) Applied external voltage V_{ex} (V_{low} = -20 V), (b) voltage applied at the external resistance V_R, (c) voltage in pentacene layer V_1 and (d) the ratio of V_1 and V_R.

4.2. Determination of carrier mobility using step-voltage

On the other hand, step-voltage is available for the determination of the transit time t_r, as discussed in Section 3.1. The advantage of using step-voltage is that we can trace the current

ΔI (the second term of Eq. (A1)) generated due to the carrier transit to the pentacene/PI interface, and can determine the carrier transit time, as discussed in the Appendix. In the experiment, it is easy to distinguish ΔI from I_0 (the first term of Eq. (A1)), because carriers cannot inject into the pentacene layer at $t = 0$ owing to the presence of potential barrier at the electrode/pentacene interface, that is $\Delta I = 0$ at $t = 0$, and the current ΔI gradually increases along with the carrier injection. The end of carrier transit can be regarded as the time when the current I was decreased to I_0 according to Eq. (A1). On the contrary, under a ramp-voltage application, transit time is difficult to be estimated from ΔI because injected carrier uniformly distributes across the conductive pentacene layer and ΔI cannot be simply expressed as a function of the position of the carrier. Therefore, we believe that using step-voltage is a much better choice for the determination of carrier transit time.

Although it was found that a step-voltage application is helpful for the determination of carrier mobility, a step voltage can be approximately expressed as $V_{ex} = V_{low} + At$ in the same way as a ramp voltage, in the limit $A \rightarrow \infty$. In other words, our result suggests that high sweep rate A is necessary to keep the pentacene layer insulating during carrier transport in order to measure carrier transport by the time they spread uniformly across the pentacene layer. We applied voltages linearly increasing from 0 V to 20 V with different sweep rates A and derived the relaxation times τ from the observed decaying current. Fig. 7 shows the relationship between sweep rates A and measured relaxation times τ. It was found that at a high sweep rate, relaxation time τ equals to the time constant $\tau_1 = R_{ex}C_1C_2/(C_1+C_2) = 42$ ns, which indicates that pentacene serves like an insulator. However, as the sweep rate decreases, relaxation time τ increases. This is possibly caused by pentacene changing its apparent electrical property from insulator to conductor, by carriers uniformly spreading across the pentacene layer. At an extremely low sweep rate A, pentacene is serving as conductor and the relaxation time is presumably expressed as $\tau_3 = (R_{ex}+R_1)C_2$, where R_1 denotes the resistance of the pentacene layer. That is, it is clear that step-voltage with high sweep rates A of around 10^9 V/s is suitable for the determination of carrier mobility of pentacene.

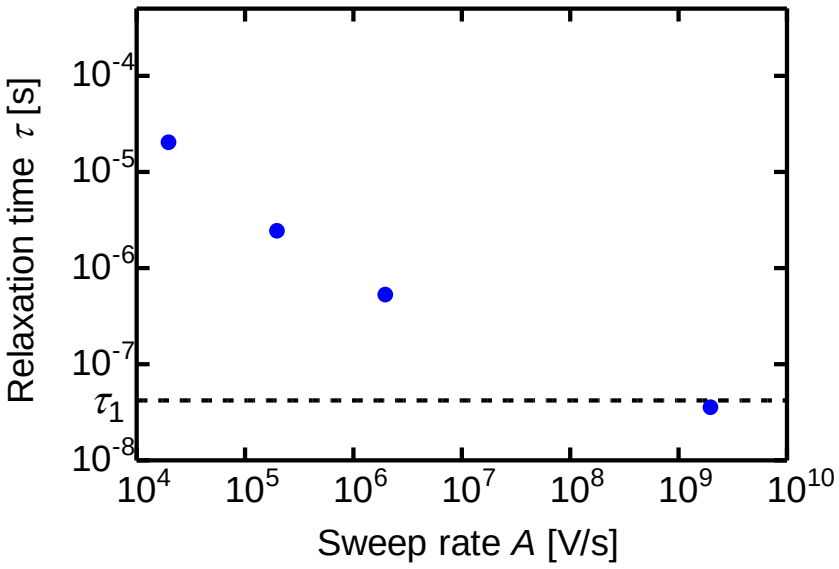

Fig. 7. The correlation between sweep rate A and relaxation time τ.

5. Conclusions

In conclusion, we proposed a method for determining carrier mobility by using DCM in combination with EFISHG measurement. EFISHG directly probes the electric field E_1 along with hole transfer in the pentacene layer, and the hole mobility μ is determined using the relationship of $\int_0^{t_r} \mu E_1 \, dt = d_1$. Furthermore, step-voltage and ramp-voltage were applied to MIS diodes. Under a step-voltage application, carrier transport and the transit time were observed in current transients, while under a ramp-voltage application, Ohmic current flew and the determination of transit time was difficult. Therefore, we concluded that step-voltage application is suitable for the determination of carrier mobility. Furthermore, this study suggests that the conventional CELIV method is incomplete and the electric field in organic layer must be directly measured in the carrier mobility measurement, e.g., by EFISHG method.

Acknowledgments

This work was financially supported by a Grant-in-Aid for Scientific Research(S) (Grant No. 22226007) from the Japan Society for the Promotion of Science (JSPS), Japan. T. N. thanks to the Tokyo Tech-Tsinghua University Joint Graduate Program.

Appendix

Model of charge sheet transport

Firstly, let us consider the current I flowing when a charge sheet transports across insulating pentacene layer under a step-voltage application. Here we define V_s, Q and $\bar{x}$ as the voltage applied at the sample, the charge amount of the charge sheet and the position of charge sheet in pentacene layer (see Fig. A1), respectively. Then current I is written as

$$I = \frac{C_1 C_2}{C_1+C_2}\frac{dV_s}{dt} + \frac{Q}{d_1}\frac{C_2}{C_1+C_2}\frac{d\bar{x}}{dt}. \quad \text{(A1)}$$

At the time before carriers inject into the pentacene layer and after they reach the pentacene/PI interface, $\frac{d\bar{x}}{dt} = 0$. That is, the current I is merely given by the first term of Eq. (A1). Therefore, the following relationship is derived.

$$R_{ex}\frac{C_1 C_2}{C_1+C_2}\frac{dV_s}{dt} + V_s = V_{ex} \quad \text{(A2)}$$

Solving (A2), we obtain the voltage applied to the sample V_s as

$$V_s(t) = V_{ex}\left\{1 - \exp\left(-\frac{t}{\tau_1}\right)\right\}. \quad \text{(A3)}$$

Here, $\tau_1 = R_{ex}\frac{C_1 C_2}{C_1+C_2} = 42$ ns. Substituting (A3) into the first term of (A1), we obtain

$$I(t) = I_0(t) = \frac{V_{ex}}{R_{ex}}\exp\left(-\frac{t}{\tau_1}\right). \quad \text{(A4)}$$

That is, without carrier transport in the pentacene layer, the flowing current corresponds to I_0 as shown in region (ii) and (iv) in Fig. 2 (c), indicating that region (iii) corresponds to transit time.

Secondly, let us consider the electric field formed in the pentacene layer when a charge sheet transports. The electric fields at both sides of a charge sheet are different due to the electric field generated from a charge sheet itself. As illustrated in Fig. A1, electric field E_{12} can be considered to convey the carrier sheet.

Here, under assumption that a charge sheet Q exists only at $x = \bar{x}$ $(0 < \bar{x} < d_1)$ and there are no charges at the pentacene/PI interface, electric flux density D is continuous at the pentacene/PI interface as follows:

$$D = \varepsilon_0\varepsilon_1 E_{12} = \varepsilon_0\varepsilon_2\frac{V_s - \overline{E_1}d_1}{d_2}. \quad \text{(A5)}$$

Here, V_s and $\overline{E_1}$ denote the voltage across the sample and the average electric field in the pentacene layer, respectively. That is, we can rewrite Eq. (A5) as

$$E_{12} = \frac{C_2}{C_1}\left(\frac{V_s}{d_1} - \overline{E_1}\right). \quad \text{(A6)}$$

Here, $V_s(= V_{ex} - R_{ex}I)$ is obtained by DCM, and $\overline{E_1}$ is directly measured by EFISHG. Accordingly, the carrier mobility is directly determined by EFISHG and DCM using the following equation

$$\mu = \frac{d_1}{\int_{t_{inj}}^{t_{inj}+t_r} E_{12}\,dt}. \quad \text{(A7)}$$

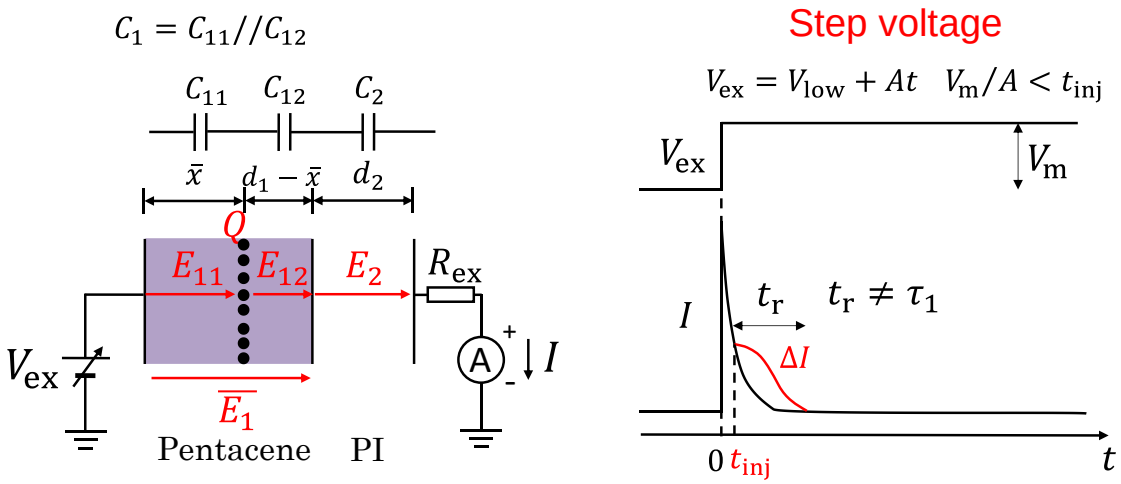

Fig. A1. The carrier transport model under a step-voltage application.

References

[1] G. Juška, N. Nekrašas, K. Genevičius, Investigation of charge carriers transport from extraction current transients of injected charge carriers, J. Non. Cryst. Solids. 358 (2012) 748–750. doi:10.1016/j.jnoncrysol.2011.12.016.

[2] G. Juška, N. Nekrašas, K. Genevičius, A. Pivrikas, Current transients in organic field effect transistors, Appl. Phys. Lett. 102 (2013) 163306. doi:10.1063/1.4803054.

[3] A. Armin, G. Juska, M. Ullah, M. Velusamy, P.L. Burn, P. Meredith, A. Pivrikas, Balanced Carrier Mobilities: Not a Necessary Condition for High-Efficiency Thin Organic Solar Cells as Determined by MIS-CELIV, Adv. Energy Mater. 4 (2014) 1300954. doi:10.1002/aenm.201300954.

[4] J. Peng, X. Chen, Y. Chen, O.J. Sandberg, R. Österbacka, Z. Liang, Transient Extraction of Holes and Electrons Separately Unveils the Transport Dynamics in Organic Photovoltaics, Adv. Electron. Mater. 2 (2016) 1500333. doi:10.1002/aelm.201500333.

[5] J. Važgėla, K. Genevičius, G. Juška, i-CELIV technique for investigation of charge carriers transport properties, Chem. Phys. (2016) 2–5.

doi:10.1016/j.chemphys.2016.04.005.

[6] Y. Gao, A. Pivrikas, B. Xu, Y. Liu, W. Xu, P.H.M. van Loosdrecht, W. Tian, Measuring electron and hole mobilities in organic systems: charge selective CELIV, Synth. Met. 203 (2015) 187–191. doi:10.1016/j.synthmet.2015.02.036.

[7] J.U. Wallace, R.H. Young, C.W. Tang, S.H. Chen, Charge-retraction time-of-flight measurement for organic charge transport materials, Appl. Phys. Lett. 91 (2007) 152104. doi:10.1063/1.2798592.

[8] S. Egusa, N. Gemma, A. Miura, K. Mizushima, M. Azuma, Carrier injection characteristics of the metal/organic junctions of organic thin-film devices, J. Appl. Phys. 71 (1992) 2042. doi:10.1063/1.351150.

[9] T. Manaka, E. Lim, R. Tamura, M. Iwamoto, Direct imaging of carrier motion in organic transistors by optical second-harmonic generation, Nat. Photonics. 1 (2007) 581–584. doi:10.1038/nphoton.2007.172.

[10] D. Taguchi, M. Weis, T. Manaka, M. Iwamoto, Probing of carrier behavior in organic electroluminescent diode using electric field induced optical second-harmonic generation measurement, Appl. Phys. Lett. 95 (2009) 263310. doi:10.1063/1.3277155.

[11] M. Iwamoto, T. Manaka, D. Taguchi, Modeling and visualization of carrier motion in organic films by optical second harmonic generation and Maxwell-displacement current, J. Phys. D. Appl. Phys. 48 (2015) 373001. doi:10.1088/0022-3727/48/37/373001.

[12] T. Noma, D. Taguchi, T. Manaka, M. Iwamoto, Analysis of Carrier Behaviors in Double-layer Organic Devices by Displacement Current Measurement and Electric-field-induced Optical Second-harmonic Generation Measurement, IEICE Trans. Electron. E98–C (2015) 86–90. doi:10.1587/transele.E98.C.86.

[13] D. Taguchi, T. Shino, L. Zhang, J. Li, M. Weis, T. Manaka, M. Iwamoto, Direct Probing of Photovoltaic Effect Generated in Double-Layer Organic Solar Cell by Electric-Field-Induced Optical Second-Harmonic Generation, Appl. Phys. Express. 4 (2011) 21602. doi:10.1143/APEX.4.021602.

[14] M. Kakimoto, M. Suzuki, T. Konishi, Y. Imai, M. Iwamoto, T. Hino, Preparation of mono- and multilayer films of aromatic polyimides using Langmuir-Blodgett technique., Chem. Lett. (1986) 823–826. doi:10.1246/cl.1986.823.

[15] Y.R. Shen, The Principles of Nonlinear Optics, New York, 1984.

[16] L. Zhang, D. Taguchi, J. Li, T. Manaka, M. Iwamoto, Probing of interfacial charging and discharging in double-layer devices with a polyimide blocking layer by time-resolved optical second harmonic generation, J. Appl. Phys. 108 (2010) 93707. doi:10.1063/1.3483929.

[17] Z. Shang, T. Heumueller, R. Prasanna, G.F. Burkhard, B.D. Naab, Z. Bao, M.D. McGehee, A. Salleo, Trade-Off between Trap Filling, Trap Creation, and Charge Recombination Results in Performance Increase at Ultralow Doping Levels in Bulk Heterojunction Solar Cells, Adv. Energy Mater. (2016) 1601149. doi:10.1002/aenm.201601149.